Fragility and Resilience Indicators for Portfolio of Oil Storage Tanks Subjected to Hurricanes

Sabarethinam Kameshwar, A.M.ASCE[1]; and Jamie E. Padgett, A.M.ASCE[2]

Abstract: This paper develops fragility functions and estimates of resilience indicators for aboveground storage tanks (ASTs) subjected to hurricanes, which can be efficiently applied to all the tanks in a regional portfolio of ASTs to assess their hurricane performance. Fragility and resilience assessment of a portfolio of ASTs is essential for planning mitigation strategies at the regional level and at the level of individual structures. Recently, studies have started assessing the fragility of ASTs under hurricane loads; most of the existing studies are focused on a specific AST type and a specific hurricane-related hazard. However, in order to facilitate performance assessment of an entire portfolio of ASTs, fragility functions for different types of tanks and hazards are necessary, which are lacking in the literature. Furthermore, estimates for resilience indicators such as repair costs and downtime are also not available in the literature. Therefore, to address these gaps, this study first develops fragility functions for different types of ASTs subjected to hurricane winds and storm surge. Next, estimates of repair costs and downtime are defined for different failure modes of ASTs by adapting costs and downtime for similar failure modes from different hazards. The fragility functions, repair costs, and downtime estimates developed herein are used to assess the performance of ASTs in the Houston Ship Chanel (HSC), which houses more than 4,500 ASTs, for two synthetic hurricane scenarios corresponding to 100 and 250-year return period events. For both scenarios, 100,000 Monte Carlo simulations are performed for each tank to determine the failure probability, repair costs, and downtime for all ASTs while propagating uncertainties in the fill level and density of contents stored in all ASTs. Furthermore, the influence of anchoring all tanks as a storm surge risk mitigation strategy on the performance of ASTs is also evaluated. The results provide several insights into the performance of tanks in the Houston Ship Channel during the two hurricanes: the tanks are not vulnerable to hurricane winds; however, failures are observed due to storm surge, which highlights the need for storm surge mitigation measures for the Houston Ship Channel region. Furthermore, tanks with the highest failure probability do not necessarily lead to high spill volumes or repair costs. Moreover, even minimum anchoring is observed to be effective in significantly reducing the spill volume and repair costs.
DOI: 10.1061/(ASCE)IS.1943-555X.0000418.

Introduction

Aboveground storage tanks (ASTs) are a key component of the infrastructure used by the petrochemical industry. Aboveground storage tanks are large cylindrical structures with thin metal walls which are primarily used for storing hazardous substances such as crude oil. The structural integrity of ASTs is essential for proper functioning of facilities such as petrochemical refineries and processing plants, which significantly contribute to the regional economy and provide employment to many people. Moreover, several studies have observed ASTs to be one of the most vulnerable components during hurricanes and floods (Cozzani et al. 2010; Godoy 2007). Therefore performance assessment of a regional portfolio of tanks, i.e., evaluation of safety, resilience indicators, and consequences of failure such as magnitude of hazardous spills for various natural hazards, is essential to support decision making for selecting regional-level and structural-level risk mitigation strategies. However, in order to assess the performance of an entire regional portfolio of tanks, which is influenced by several sources of uncertainties, fragility models are required for different types of types of tanks and hazards. Moreover, estimates of parameters that indicate the resilience of the infrastructure, such as downtime and economic losses, and estimates of the magnitude of the hazardous spill volume are also needed. However, these estimates are not available in the literature for hazards such as hurricanes, even though catastrophic tank failures have been observed during past hurricane and flood events. During Hurricanes Katrina and Rita, a large number of tanks buckled due to high wind pressure, and several tanks floated away due to storm surge (Godoy 2007). An oil spill caused by flotation failure of just one large AST left more than 1,700 homes uninhabitable and cost more than $300 million in clean-up and litigation costs (NBCNews.com 2006). Such spills not only adversely impact the surrounding environment (Kingston 2002; Maki 1991), but they also severely impact the physical and mental wellbeing of surrounding populations (Palinkas et al. 1993). In spite of such failures, past studies have primarily developed probabilistic performance assessment tools for ASTs subjected to earthquakes, and the literature is lacking such tools for hurricane-related hazards.

Several studies have evaluated the performance of ASTs subject to earthquakes (Barton and Parker 1987; Haroun and Housner 1981; Niwa and Clough 1982; Sakai et al. 1984) and developed fragility models for a regional portfolio of tanks (Fabbrocino et al. 2005; Salzano et al. 2003). Furthermore, HAZUS-MH (NIBS 2005) provides functions that estimate direct costs and downtime for various types of seismic damage to ASTs. However, such fragility functions and estimates for economic loss and downtime are not available for hurricane-related hazards such as storm surge and

[1]Graduate Research Assistant, Dept. of Civil and Environmental Engineering, Rice Univ., 6100 Main St., MS-318, Houston, TX 77005. ORCID: https://orcid.org/0000-0003-0205-8022. E-mail: sabarethinam.kameshwar@gmail.com

[2]Associate Professor, Dept. of Civil and Environmental Engineering, Rice Univ., 6100 Main St., MS-318, Houston, TX 77005 (corresponding author). E-mail: jamie.padgett@rice.edu

Note. This manuscript was submitted on November 22, 2016; approved on September 26, 2017; published online on January 26, 2018. Discussion period open until June 26, 2018; separate discussions must be submitted for individual papers. This paper is part of the ***Journal of Infrastructure Systems***, © ASCE, ISSN 1076-0342.

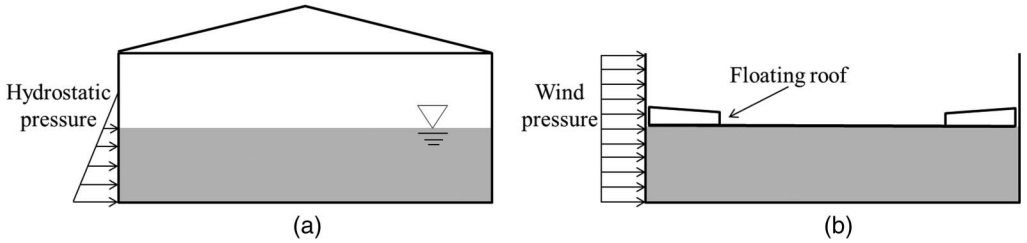

Fig. 1. Schematic representation of (a) fixed-roof tanks; (b) floating-roof tanks

wind. Kameshwar and Padgett (2018) identified flotation and buckling as primary failure modes for tanks subjected to storm surge and developed fragility functions that can be efficiently applied to a portfolio of ASTs. However, the buckling fragility functions were developed for tanks with fixed roofs and cannot be applied to tanks with floating roofs, which are commonly found in industrial complexes, due to differences in the structural characteristics of the two types of ASTs. Fig. 1 shows schematic representations of fixed and floating-roof tanks along with a schematic representation of wind and surge loads. Fixed roof tanks have different roof shapes, such as conical (Fig. 1) and spherical, which are fixed at the top of the tank and are usually supported by columns inside the tank. However, floating-roof tanks have roofs that float over the contents of the tank and are able to move freely along the height of the tank. Studies in the literature have not assessed storm surge buckling fragility for these structures.

Apart from storm surge, strong winds during hurricanes have also caused buckling damage to tanks, which affects the functionality of ASTs. Existing studies on the performance of ASTs subjected to wind pressure deterministically determined the wind buckling capacity of ASTs (Flores and Godoy 1998; Portela and Godoy 2005a, b; Zhao and Lin 2014). Kameshwar and Padgett (2015a) demonstrated the presence of significant uncertainty in wind buckling capacity of ASTs. However, the literature lacks studies that can facilitate efficient wind buckling fragility assessment for ASTs with different roof types. Furthermore, the literature also lacks estimates of repair cost and downtime estimates for storm surge–related and wind-related AST failures.

In order to address these gaps, this study first develops wind buckling fragility functions for fixed roof tanks. For this purpose, finite-element simulations are performed for a large number of tanks with different geometric and design parameters to evaluate the buckling capacity of ASTs. Based on the results of the finite-element simulations, metamodels are trained to predict buckling failure of ASTs for given tank parameters and the hazard intensity measure, wind speed. Additionally, a logistic regression model is also developed, using the output from the trained metamodel, to directly predict the probability of failure. For tanks with floating roofs, this study models the radial stiffness of the rim seal in floating roofs with springs in radial directions. Furthermore, because the actual radial stiffness of the rim seal is unknown, a sensitivity analysis is performed to evaluate its effect on the buckling performance of ASTs. Following the sensitivity analysis, buckling fragility functions for floating-roof tanks subjected to hurricane wind and storm surge are developed using the procedure adopted for fixed roof tanks. Next, resilience indicators such as downtime and repair costs are developed for hurricane-related failures based on available data for seismic failures considering the similarities in the different failure modes during earthquakes and hurricanes. These estimates of resilience indicators and fragility functions along with flotation fragilities adapted from Kameshwar and Padgett (2018) are used to assess hurricane performance of the portfolio of tanks in the Houston Ship Channel (HSC), which has more than 4,500 tanks, for two synthetic storms.

Fragility Functions for Fixed Roof Tanks

Past reconnaissance studies and flood preparedness guidelines by the United States Environmental Protection Agency have identified buckling of tank shells due to wind, flotation due to storm surge, buckling of tank shells due to storm surge, and debris impact as the major causes of damage to tanks (Cozzani et al. 2010; EPA 2016; Godoy 2007). Therefore this study considers flotation and buckling due to wind and surge for performance assessment of AST. This study does not consider debris impact due to lack of information on the amount and type of debris generated in industrial areas; however, future work will focus on performance assessment of ASTs subjected to debris impact. This study first develops fragility functions for wind buckling, which are currently lacking, and adopts existing fragility functions for storm surge–related failures for fixed-roof ASTs. Specifically, this section focuses on fragility assessment of fixed roof tanks, which usually constitute the majority of ASTs in a regional portfolio.

Wind Buckling Fragility

Strong winds during hurricanes exert excessive pressure on tank shells, which causes instability in the tank shell and ultimately leads to buckling. In most cases, buckling leads to deformations in the tank shell. In cases in which buckling only causes elastic deformations, the buckled sections may be repaired by simply pulling on the deformed section of the shell to bring it back to its original undeformed shape. When buckling leads to inelastic deformation, the buckled section of the shell needs to be replaced to repair the tank. Buckling of the tank shell influences the immediate postevent functionality of tanks and also leads to direct and indirect economic losses. Buckling performance of ASTs is influenced by several factors such as the strength of tank shell, level of fill inside the tank providing resistance against buckling, density of the contents, dimensions of the tank, and wind speed. Therefore these parameters were considered as variables for wind buckling fragility assessment of ASTs. Table 1 shows the range of these variables considered in this study; L is the height of the product stored inside the tank, V is

Table 1. Range of Tank Parameters Considered in Buckling Fragility Analysis

Parameter	Description	Lower bound	Upper bound
D (m)	Diameter	5.0	70.0
ρ_l	Relative density of contents	0.5	1.0
L (m)	Fill level	0.0	$0.9H$
V (m/s)	Wind speed	0.0	300.0
S_d (MPa)	Product design stress	137.0	196.0

wind speed, ρ_l is the density of contents relative to the density of water, and S_d is the product design stress which determines the maximum allowable stress on the tank shell due to the presence of the tank's contents. Therefore, a larger value of S_d would lead to thinner shells and a smaller value of S_d would lead to thicker shells. The range of S_d values in Table 1 was obtained based on the range of S_d values prescribed in American Petroleum Institute (API) Guideline 650 (API 2013) for different materials that may be considered for AST shells. Tank height (H), not shown in Table 1, was assumed to be correlated to tank diameter (D), as observed from the analysis of tank dimensions for more than 4,000 tanks in the Houston Ship Channel. Based on this analysis, the lower and upper bounds for tank aspect ratio (H/D) were derived as $\exp(0.25 - 0.5 \ln D)$ and $\exp(3.07 - 0.95 \ln D)$, respectively. For each tank with a given diameter, the tank height was obtained by randomly selecting an aspect ratio within the bounds of aspect ratio and multiplying it by tank diameter.

In order to efficiently span the range of variables shown in Table 1 along with tank height, this study used Latin hypercube sampling (LHS) to generate 1,800 combinations of tank parameters. For each combination of parameters, a tank was designed in accordance with API 650 design guidelines (API 2013) and modeled in *LS-DYNA* (Hallquist 2012), a finite-element program. The tank shell was modeled using 0.25×0.25-m-square thin shell elements. The size of the elements was chosen based on a mesh convergence study. Fixed boundary conditions were provided at the base of the tank shell, similar to past studies (Flores and Godoy 1998; Godoy and Flores 2002; Portela and Godoy 2005b). The finite-element modeling approach was validated by comparing the eigenvalues of the tanks modeled by Virella et al. (2003). For further validation, the buckling and postbuckling performance of several ASTs were compared against results reported by Portela and Godoy (2005a). These comparisons provided confidence in the modeling approach used in this study. Kameshwar and Padgett (2015a, b) provided additional details on tank modeling. The finite-element modeling of ASTs also incorporated geometric imperfections on the tank shell which significantly affect the buckling response of shell structures such as ASTs (Teng and Rotter 2006). For this purpose, the generalized imperfection modeling scheme proposed by Kameshwar and Padgett (2015a) was used. The imperfection modeling methodology uses a two-dimensional Fourier series with random coefficients to model the imperfections in tank shells. Buckling analysis was performed for each parameter combination to determine the minimum wind pressure and the corresponding critical wind speed (V_{cr}) that initiates buckling of the tank shell. For this purpose, the wind pressure distribution on tanks was obtained from Eurocode EN 1993-4-1 (CEN 2007), which provides estimates of wind pressure distribution based on experimental results as a function of AST height and diameter. Herein, the finite-element simulations used to evaluate V_{cr} neglected the dynamic effects of wind loads because these effects have insignificant effect on the wind buckling capacity of ASTs (Flores and Godoy 1998).

In order to facilitate fragility assessment, the critical wind speed for each tank was compared with the assigned wind speed V to determine if the tank failed, generating a binary output for each simulation of 1 for fail and 0 for safe. This binary output was used as an input to the dual-layer metamodel-based fragility assessment (DL-MFA) methodology (Kameshwar and Padgett 2018), which was adapted herein for fragility assessment of ASTs under wind loads and storm surge. The DL-MFA methodology adopted herein is an improvement over the conventional limit state–based approaches such as the first-order reliability methods which provide valuable information but cannot be used for developing parameterized fragility models or for noisy limit states. Furthermore, Monte Carlo simulation (MCS)-based approaches are computationally expensive. The DL-MFA methodology addresses these challenges. Therefore, following the DL-MFA methodology, the binary output was used to train different metamodels to predict the failure of ASTs. For this purpose, this study considered several metamodels, such as support vector machines (Cristianini and Shawe-Taylor 2000), random forest (Pavlov 2000), and logistic regression (Hosmer and Lemeshow 1989). Among the three metamodels, the best metamodel, based on prediction accuracy, was selected to train the second metamodel, logistic regression, which was used for fragility assessment. For this purpose, 10×10^4 tank parameter combinations were generated using LHS, and for each parameter combination the first metamodel was used to predict the failure of the AST. This binary output and the 10×10^4 tank parameter combinations were used to train the final logistic regression model. Kameshwar and Padgett (2018) presented additional details, along with a flowchart, on the DL-MFA methodology. The trained logistic regression model can be used to obtain the binary output as well as to determine the probability of failure. This approach yields a logistic regression model which retains the accuracy of the first metamodel and has narrower confidence bounds for failure probability predictions. This study used the stepwise logistic regression methodology, which adds parameters and their combination if an improvement in the logistic regression model is observed, leading to a sparse logistic regression model. Herein, the final logistic regression model, trained on a random forest metamodel, had an accuracy of 94.97% for classification; the test set consisted of 200 AST parameter combinations whose performance was obtained using finite-element simulations. The logistic regression model can also be used to obtain the probability of failure as

$$P(wind\ buckling|D, H, V, \rho_l, L, S_d) = \frac{1}{1 + \exp\left[-g_{wb}(D, H, V, \rho_l, L, S_d)\right]} \tag{1a}$$

where

$$\begin{aligned} g_{wb}(D, H, V, \rho_l, L, S_d) = {} & -2.82 - 0.55D + 0.32H + 5.14 \\ & \times 10^{-2}V - 1.83\rho_l - 1.48 \times 10^{-1}L \\ & + 1.17 \times 10^{-2}DH + 6.96 \times 10^{-3}DV \\ & + 3.93 \times 10^{-3}HV - 4.47 \times 10^{-3}D^2 \\ & - 2.19 \times 10^{-2}H^2 \end{aligned} \tag{1b}$$

where $g_{wb}(D, H, V, \rho_l, L, S_d)$ = logit function for wind buckling, which predicts the logarithm of the odds of wind buckling. Table 1 defines the symbols used in Eqs. (1*a*) and (1*b*). The failure probability predicted by Eq. (1*a*) can be rounded off to obtain the binary output, if desired. The logistic regression model in Eq. (1) can be used to efficiently predict wind buckling failure for a large number of tanks without any finite-element simulations. Such a format is particularly attractive for risk and resilience modeling of a portfolio of tanks with a range of design and geometric parameters.

Storm surge Flotation Fragility

Flotation failure of ASTs is governed by Archimedes' principle; i.e., the tank fails due to flotation if the buoyancy forces exceed the total self-weight of the tank. In the case of anchored tanks, the anchors provide additional resistance against flotation. This paper neglected hydrodynamic load effects due to the speed of the incoming surge and potential wave loads because *ADCIRC* (Luettich and Westerink 2004) simulations of potential storms showed that on

land where tanks are located the velocities and wave heights are typically relatively low, less than 0.5 m/s and 0.3 m, respectively. However, ongoing and future research will address the additional complexities introduced when considering such phenomena. In order to predict flotation failure of unanchored and anchored tanks, this study used the logistic regression models developed by Kameshwar and Padgett (2018); the logit function for the flotation failure of unanchored tanks is

$$g_{sua}(D,H,L,S,\rho_l) = -8.67 + 0.43D - 0.64H - 0.10L - 3.14\rho_l + 39.53S - 38.47L\rho_l - 4.47\times10^{-3}D^2 \quad (2)$$

where g_{sua} = logit function for storm surge flotation for unanchored tanks; and S = depth of inundation caused by storm surge. In order to obtain the failure probability, the logit function in Eq. (2) can be used in the same manner that Eq. (1*b*) is used along with Eq. (1*a*). The accuracy of the logistic regression model in Eq. (2) was 99.9% on a test set containing 1,000 parameter combinations. The logit function for anchored tanks, which had an accuracy of 97.3% and consists of more than 50 terms, is not shown here for brevity.

Storm Surge Buckling Fragility

Tanks that are restrained from floating away either due to the presence of anchors or due to the local topography may buckle due to the large hydrostatic pressure created by storm surge inundation. For buckling analysis, similar to flotation analysis, hydrodynamic loads and potential wave loads are neglected and buckling analysis is performed considering hydrostatic loads only. Past studies have shown that at high inundation levels anchored tanks are more vulnerable to buckling than to flotation (Kameshwar and Padgett 2015b, 2018). Storm surge buckling failure may rupture the tank shell near the joints for pipelines and may lead to spills. Therefore this study considered storm surge buckling while evaluating the performance of ASTs during hurricanes, and obtained the logit function for storm surge buckling from Kameshwar and Padgett (2018). The logit function for storm surge buckling, $g_{sb}(D,H,L,S,\rho_l,S_d)$, which had an accuracy of 95.4% on a test set consisting of 200 AST parameter combinations, is

$$\begin{aligned} g_{sb}(D,H,L,S,\rho_l,S_d) = {} & -46.72 + 4.55D + 0.87H - 3.10S \\ & - 16.76\rho_l + 1.81L + 6.50\times10^{-2}S_d \\ & - 2.08\times10^{-2}DH + 1.50SH - 0.40HL \\ & - 0.18D^2 - 0.30H^2 - 4.71\times10^{-2}H^2S \\ & + 1.5\times10^{-2}H^2L + 3.06\times10^{-3}D^3 \\ & + 9.8\times10^{-3}H^3 - 1.85\times10^{-5}D^4 \end{aligned} \quad (3)$$

The fragility functions in Eqs. (1)–(3) enable rapid fragility assessment of fixed-roof ASTs subjected to hurricane winds and storm surge. This study develops such currently lacking fragility functions for floating-roof tanks in the following section.

Fragility Functions for Floating-Roof Tanks

Floating-roof tanks are commonly found in tank farms and industrial facilities. They are primarily used to store volatile substances in order to reduce vapor loss and avoid accidental fire and blast incidents due to ignition of the vapors. For this purpose, the roof of the tank is designed to float over the liquid stored in the tank, and therefore it is not directly connected to the tank's shell. The roof and the tank shell are connected through a rim seal provided around the circumference of the floating roof to prevent loss of vapors in to the atmosphere and to allow easy movement of the roof along the height of the tank. The rim seal consists of several components such as a sealing ring, a flexible seal, and a hangerlike mechanism that connects the roof to the sealing ring which is in contact with the tank shell. Myers (1997) provided additional details on floating-roof tanks. Fig. 2 presents a schematic diagram of a pantograph-type rim seal, which is one of the several types of rim seals used in floating-roof ASTs. The presence of the floating roof and the connecting rim seal may influence the buckling response of ASTs under hurricane loads. Therefore separate fragility curves are necessary to evaluate the buckling performance of ASTs with floating roofs. Because fragility functions for floating tanks are not available in the literature for wind and storm surge induced loads, this study proposes new fragility models.

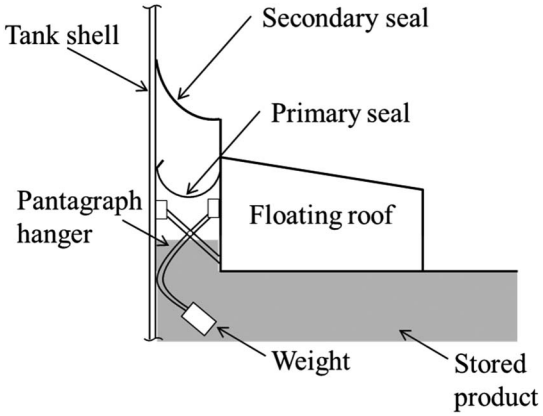

Fig. 2. Schematic diagram of a pantograph-type rim seal (adapted from Myers 1997)

Wind Buckling Fragility

The buckling response of floating-roof ASTs may be influenced by the set of parameters considered for wind buckling of fixed-roof ASTs: tank dimensions, liquid level, relative density of contents, product design stress, and wind velocity. In addition to these parameters, the characteristics of the rim seal may also influence the buckling response of ASTs with floating roofs. However, information on the characteristics of rim seal such as stiffness, which may vary among tanks, is not available in the literature. Furthermore, only a few studies have modeled the floating roof along with the rim seal. Hosseini et al. (2011) performed seismic analysis of a floating-roof tank in which they modeled the rim seal with discrete radial springs provided at 5° intervals, each having a stiffness of 1,500 kN/m. This stiffness value was reported for a tank with a 109-m diameter, i.e., the radial stiffness of the seal was considered to be 315 kN/m/m. Alternative estimates for the stiffness of rim seals of different sizes and types are not available in the literature. Therefore, this study performed a sensitivity analysis to study the effect of the rim seal stiffness on the wind buckling performance of ASTs by varying the rim seal stiffness value by two orders of magnitude. For this purpose, analysis of variance was performed on the buckling response, i.e., the critical wind speed causing buckling. For ANOVA, three levels (low, medium, and high) were chosen for D, L, ρ_l, S_d, and the seal stiffness, k_{seal}. The low and high values for D, L, ρ_l, and S_d were chosen as the minimum and maximum values, respectively, of the ranges of these variables in Table 1; the medium value was chosen as the mean of the low and high values.

The low, medium, and high values for k_{seal} were chosen as 40, 400, and 4,000 kN/m/m, which covers a range of k_{seal} which is an order of magnitude lower and higher than the value reported by Hosseini et al. (2011). Three values for the five variables resulted in 3^5 combinations; for each combination, a finite-element model was created and the roof was modeled using radial springs with one end attached to the tank shell and other end fixed, assuming rigidity of the floating roof in the radial direction. Subsequently, buckling analysis was conducted for all 243 combinations to evaluate the critical wind speed and ANOVA was performed. Table 2 shows the results of analysis of variance, including p-values corresponding to each of the parameters and their interaction terms. Low p-values, close to zero, indicate that variation in the corresponding variable led to significant differences in the response (critical wind velocity). Most of the variables except S_d had low values. Although S_d itself may not have a significant effect, its interaction with other variables such as D had significant effect, so S_d should be considered for the fragility analysis. Stiffness of the seal and many of its interaction terms also had low p-values. This observation implies that stiffness of the rim seal may have a significant effect on the wind buckling response of ASTs.

Because ANOVA results suggest that seal stiffness may be an important variable, this study included k_{seal} as a variable for assessing the fragility of floating-roof ASTs. This study used the dual-layer metamodel strategy, used for wind buckling analysis of fixed-roof tanks, to develop wind buckling fragility functions for floating-roof tanks. In addition to the variables in Table 1, k_{seal} was also considered for the fragility analysis with lower and upper bound values of 40 and 4,000 kN/m/m, respectively. Using LHS, 1,800 parameter combinations were created and finite-element simulations were performed for each parameter combination to obtain critical wind speeds. Comparison of V_{cr} with V resulted in the binary output which was used in the dual-layer metamodeling strategy. Herein, random forest was selected as the first metamodel and used to develop the final logistic regression model, which had 91.5% accuracy. The logit function for wind buckling of floating-roof tanks, g_{wbf}, is

$$g_{wbf}(D,H,V,L,S_d) = 5.72 - 2.29\times10^{-2}D - 1.28H - 7.18\times10^{-2}V + 7.56\times10^{-2}L - 2.06\times10^{-2}S_d + 8.14\times10^{-4}DV + 1.55\times10^{-2}HV - 3.66\times10^{-3}VL \quad (4)$$

Because the logistic regression model was developed in a stepwise manner, only the most influential parameters were included in the final logit function. Although ρ_l and k_{seal} were observed to influence the buckling response, they were not included in the final logit function when the full set of potential random variables were considered and the critical buckling wind speed was compared to a random wind speed. The simulations for ANOVA were performed without considering the effects of imperfections on the tanks shell. However, the finite-element simulations for the fragility analysis were performed considering the effect of imperfections, which led to significant uncertainty in the buckling response. Therefore exclusion of ρ_l and k_{seal} from the logit function implies that the effect of these variables on buckling performance is less than the uncertainties in buckling response caused by the presence of geometric imperfections on the tank shell. The logistic regression model corresponding to Eq. (4) was used in the following sections to perform fragility analysis of a portfolio analysis of ASTs.

Table 2. Results of Analysis of Variance for Wind Buckling Response

Parameter	p-value	
	Wind buckling	Storm surge buckling
D	0.00	0.00
ρ_l	0.00	0.00
L	0.00	0.00
S_d	0.51	0.00
k_{seal}	0.00	0.06
$D\times\rho_l$	0.97	0.00
$D\times L$	0.00	0.00
$D\times S_d$	0.00	0.00
$D\times k_{seal}$	0.00	0.05
$\rho_l\times L$	0.00	0.00
$\rho_l\times S_d$	0.58	0.27
$\rho_l\times k_{seal}$	0.95	0.77
$L\times S_d$	0.97	0.09
$L\times k_{seal}$	0.00	0.02
$S_d\times k_{seal}$	0.51	0.94

Storm Surge Flotation Fragility

The main source of difference in the flotation behavior of ASTs with fixed-roof and floating-roof tanks would arise from the difference in the weight of the roof. Floating roofs may have larger self-weight than fixed roofs. However, the combined weight of the tank shell and the roof is usually a small fraction of the total self-weight of the tank including the contents (less than 5%). Primary resistance against flotation is provided by the weight of the liquid stored in the tank and anchors, if any. Hence the self-weight of the tank roof contributes negligibly to the overall resistance against flotation, and the minimal differences that derive from roof type are insignificant. Moreover, compared with the buoyancy forces, the weight of the tank shell and roof are negligible. Therefore this study used the same fragility function for flotation failure of ASTs with fixed and floating roofs for both unanchored and anchored tanks.

Storm Surge Buckling Fragility

Storm surge buckling response, like wind buckling response, of ASTs with floating roofs may also be influenced by the presence of the floating roof. Therefore this study performed a sensitivity analysis to assess whether the stiffness of the seal rim affects the storm surge buckling response of ASTs. The 243 parameter combinations used to perform sensitivity analysis for wind buckling were used for storm surge buckling as well. For each parameter combination, the minimum storm surge that causes buckling, critical surge height, H_{cr}, was evaluated. Analysis of variance was performed on the H_{cr} values to determine if k_{seal} affects buckling response. Table 2 shows the p-values corresponding to all of the parameters and their interactions. Unlike the wind buckling analysis, k_{seal} alone did not have a significant effect on H_{cr} at a 5% confidence level; however, several interaction terms with k_{seal} had low p-values. Therefore k_{seal} was considered as a variable in the fragility analysis. The dual-layer metamodeling procedure used to derive the wind buckling fragility of floating-roof ASTs was also used to derive the fragility functions for storm surge buckling. Herein, a support vector machine model was chosen as the first metamodel, which was further used to train the logistic regression model, which had 94.0% accuracy. The logit function for storm surge buckling of floating-roof tanks (g_{sbf}) for the final logistic regression model is

$$g_{sbf}(D,H,L,S,\rho_l,S_d) = -19.69 + 0.19D - 0.18H + 1.70S + 33.91\rho_l + 1.57L - 4.90\times10^{-2}S_d - 1.86\times10^{-2}DH + 1.10\times10^{-2}DS - 0.21D\rho_l + 1.65\times10^{-3}DS_d + 7.78\times10^{-2}HS + 0.34H\rho_l - 3.77\times10^{-2}HL + 3.72\times10^{-3}HS_d + 1.04V\rho_l + 0.12SL - 1.35\rho_l L - 4.38\times10^{-3}LS_d - 0.19S^2 - 1.89\times10^{-3}D^2 - 2.46\times10^{-2}H^2 - 25.15\rho_l^2 - 0.11S_d^2 \quad (5)$$

The logit function does not include k_{seal}, even though the variation in seal stiffness may have significant effect on H_{cr}. This observation may be attributed to the limited influence of variation in seal stiffness on H_{cr} compared with the effect of other variables and the inherent variability in H_{cr} due to the presence of geometric imperfections. These findings are similar to the observations for wind buckling of floating-roof tanks. The fragility functions developed in this section address the lack of fragility functions for floating-roof tanks. These fragility functions, along with estimates of resilience indicators developed in the following section, were used for performance analysis of a regional portfolio of tanks.

Comparison of Fragility for Case Study Tanks with Different Roof Types

The flotation fragility for fixed-roof and floating-roof tanks were expected to be similar because the resistance of ASTs against flotation is not significantly influenced by roof type. Figs. 3 and 4 compare the wind and storm surge buckling fragilities, respectively, for a case study tank considering different roof types. The case study tank was 15.0 m in diameter, had a height of 10.0 m, and contained a liquid with relative density of 0.75; the dimensions corresponding to the case study tank are typically observed among the tanks in the Houston Ship Channel. Fig. 3 compares the wind buckling fragility of the case study tank with different roof types.

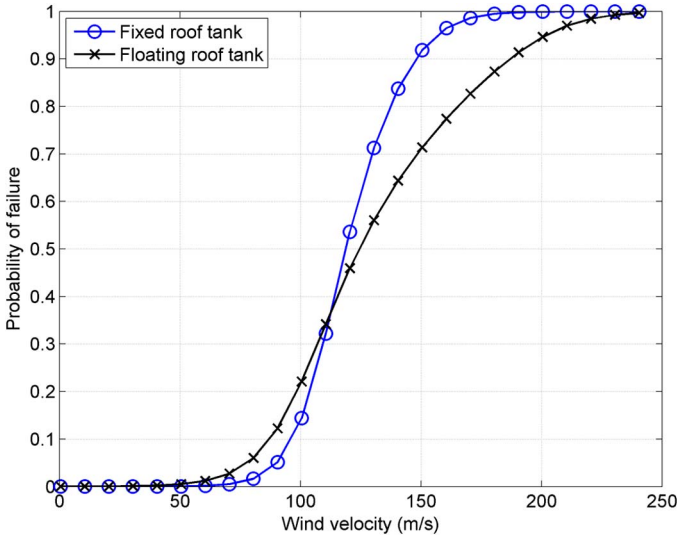

Fig. 3. Comparison of wind buckling fragility of the case study tank with fixed and floating roofs

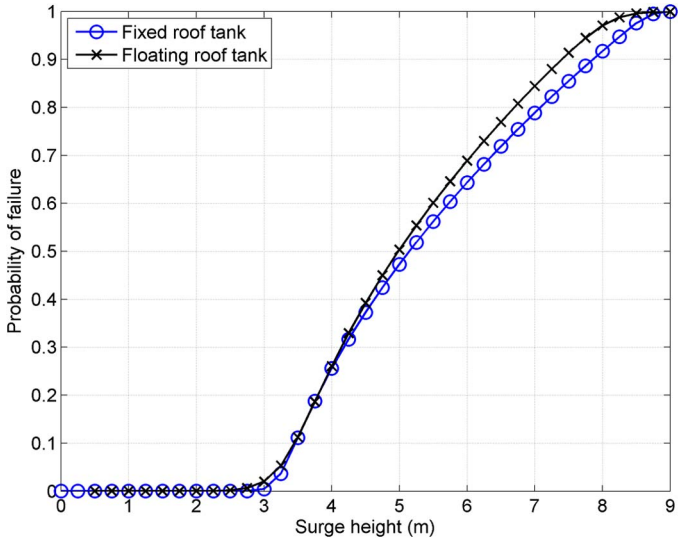

Fig. 4. Comparison of surge buckling fragility of the case study tank with fixed and floating roofs

The overall behavior of the case study tank for different roof types was similar. Moreover, the median wind speed for buckling was very close for the two roof types; however, the presence of the floating roof added significant uncertainty in the fragility. Although the variation in stiffness of the sealing ring in the floating-roof tanks was not observed to cause significant changes in the buckling behavior, the presence of the floating roof increased the buckling resistance of the case study tank. This observation could be attributed to the additional stiffness contributed by the floating-roof tank. Fig. 4 shows the storm surge buckling fragility for the tank with fixed and floating roof. Unlike wind buckling, the surge buckling behavior of ASTs was not significantly affected by the presence of the floating roof. This observation is related to the location of buckling caused by storm surge. Unlike wind buckling (in which the top shell courses buckle), surge buckling occurs at the lower shell courses, where the product stored in the tank contributes significantly to the stiffness of the tank and the additional stiffness of the floating roof does not significantly alter the stiffness of the tanks shell that experiences buckling. Therefore, for storm surge buckling, the fragility curves for the two roof types were close to each other, indicating that the difference in roof type did not significantly affect the fragility for the case study tank. The observations from Figs. 3 and 4 are specific to the selected case study tank. However, the fragility functions developed in this study can be used to facilitate such comparisons for tanks with different dimensions.

Resilience Indicators

Resilience of infrastructure systems can be defined as their capability to anticipate and absorb the effects of disruptive events, and to adapt to and recover from the outcomes of disruptive events (Berkeley III and Wallace 2010). Resilience for engineering systems is often quantified by evaluating the area under the functionality curve during the restoration period (Bruneau et al. 2003). In the case of tanks, the functionality is assumed to have two discrete states: either fully functional or completely down. This assumption is reasonable because ASTs are operated only when their structural integrity is uncompromised. Failure modes such as buckling and flotation pose a significant threat to the structural integrity of ASTs. Therefore failure of ASTs due to either flotation or buckling, due to

Table 3. Repair Cost and Downtime Estimates for Hurricane Damage

Failure mode	Downtime/repair time (days)			Damage ratio		
	Distribution	Mean	Standard deviation	Distribution	Lower bound	Upper bound
Wind buckling	Normal	3.1	2.7	Uniform	0.15	0.40
Storm surge flotation	Normal	155.0	120.0	Uniform	0.80	1.00
Storm surge buckling (without shell rupture)	Normal	3.1	2.7	Uniform	0.15	0.40
Storm surge buckling (with shell rupture)	Normal	93.0	85.0	Uniform	0.40	0.80

wind or storm surge, is assumed to cause a 100% drop in functionality. During rehabilitation, ASTs are not used; therefore, downtime for tanks may be used to indicate the resilience of ASTs. Additionally, resilience of ASTs may also be quantified in terms of economic losses and potential spill volumes due to tank failures, which indicate the potential economic and environmental impact of tank failures. Therefore this study evaluated the three resilience indicators—downtime, direct economic losses, and spill volumes—to assess the performance of ASTs in a regional portfolio of tanks.

The literature lacks downtime and repair cost estimates for tanks damaged due to various hurricane-related failure modes. Therefore for hurricane-related damage modes, this study adapted estimates for these resilience indicators from other hazards based on similarity of failure modes. Wind buckling of ASTs is usually observed to cause buckling in the upper shell courses of tanks (Godoy 2007). Furthermore, only extreme cases of wind buckling may lead to spillage of contents. This damage description matches well with consequences of moderate seismic damage to tanks as per HAZUS loss estimation methodology (NIBS 2005) and O'Rourke and So (2000), which characterized moderate damage by either elephant foot buckling with minor loss of contents or buckling in upper courses. Therefore, in order to estimate downtime and repair cost for wind buckling damage to fixed-roof and floating-roof tanks, this study adopted the repair time and loss estimates corresponding to the moderate damage state. Table 3 shows the distribution of restoration time and damage ratio, i.e., repair costs as a fraction of tank cost, for wind buckling of tanks.

Flotation failure of tanks can lead to dislocation of the tanks and rupturing of pipelines connected to the tanks. Furthermore, dislocation may also cause ruptures in the bottom shell courses, leading to complete loss of contents. Therefore flotation failure may be considered equivalent to the complete damage state for earthquake damage as per HAZUS (NIBS 2005), which is characterized by complete tank failure. Table 3 shows the distribution of damage ratio and downtime, corresponding to flotation failure of fixed-roof and floating-roof tanks, obtained from HAZUS (NIBS 2005). Storm surge buckling of ASTs is triggered when ASTs are not free to float due to the presence of restraints such as anchor bolts. Storm surge buckling, similar to wind-related buckling, may simply cause buckling without any ruptures. However, because storm surge buckling is more likely to be caused in the lower shell courses, storm surge buckling may also lead to rupture of the shell near connections with pipelines. Therefore storm surge buckling has the potential to cause ruptures in the tank shell which may cause spills. Because of a lack of data on storm surge buckling, both scenarios—buckling without and with rupture—were assumed to be equally likely. This assumption may be easily revised in the future if more data on storm surge buckling becomes available either through reconnaissance reports or experimental testing. Buckling without rupture is similar to wind buckling; therefore repair costs and downtime were considered to be the same as wind buckling. For storm surge buckling with a ruptured shell, the damages are comparable to extensive seismic damage which includes loss of contents due to elephant foot buckling and breakage of pipelines. In view of similar damages, repair costs and downtime for extensive seismic damage from HAZUS were adopted for storm surge buckling with a ruptured shell for tanks with both roof types (Table 3). For all failure modes, HAZUS provides the repair cost estimates in terms of damage ratios. In order to evaluate repair costs using damage ratios, the cost of new tanks were obtained from the Michigan tax assessors' manual (Michigan Department of Treasury 2003). However, the tax assessors' manual provides costs of tanks in 2003 U.S. dollars; therefore, the Nelson-Farrar Refinery Construction Index (2004, 2016) was used to convert the cost of tanks to present costs. Fig. 5 shows the cost curve for year 2016, i.e., the relation between cost and capacity of tanks, for fixed-roof and floating-roof tanks. For each of the failure modes which may potentially lead to spills, this study assumed that the entire contents of the tank were spilled, which is a conservative assumption. However, considering the consequences of spills the conservative assumption may be justified.

The fragility functions and the estimates of resilience indicators developed in this study provide potential opportunities for regional level resilience assessment of ASTs subjected to hurricanes. Furthermore, the tools developed in this study can also be used for performance assessment of an entire portfolio of regional ASTs subjected to hurricanes in order to inform regional-level planning and mitigation strategies. Additionally, the resilience estimates can also be used for cost-benefit analysis to determine structural-level mitigation strategies. This study applied the fragility functions and the resilience estimates to the entire portfolio of ASTs in the Houston Ship Channel to assess their hurricane performance.

Application to Houston Ship Channel

The Houston Ship Channel is one of the busiest ports in the United States. Economically, its impact is estimated at $264.9 billion, and the HSC also contributes more than 1 million jobs in the state of

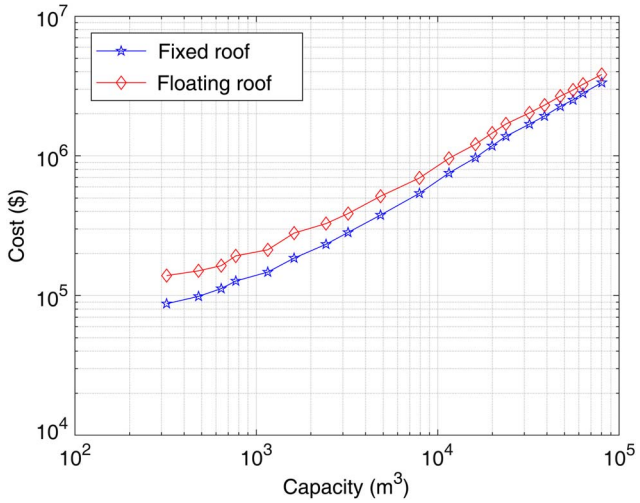

Fig. 5. Cost curve for fixed-roof and floating-roof tanks

J. Infrastruct. Syst., 2018, 24(2): 04018003

Texas (The Port of Houston Authority 2016). Furthermore, the largest petrochemical complex in the United States, the second largest in the world, is also located in the Ship Channel. As a consequence, there are more than 4,500 ASTs in the Ship Channel which may be susceptible to hurricane-related hazards, because the HSC is located on the Gulf Coast. Considering the contributions of the HSC to the regional economy and the potential economic and environmental impacts in the event of a hurricane, probabilistic risk assessment of ASTs is essential to assess the threats and determine mitigation measures. Therefore this study performed probabilistic performance assessment of the entire regional portfolio of ASTs in the HSC. For this purpose, this study first obtained information—location of tanks, their dimensions, ground elevation at tank locations, and contents stored in tanks—for all the tanks in the Ship Channel from the database of information on tanks created by Bernier et al. (2016). The database includes 4,599 tanks from the Ship Channel, of which 4,157 tanks have a fixed roof, 389 have a floating roof, and 53 tanks have an open roof, i.e. no roof. Because only approximately 1% of tanks in the HSC have open roofs, this study mainly focused on fixed-roof and floating-roof tanks. Next, two synthetic hurricanes scenarios were considered to evaluate the probabilistic performance of the portfolio of tanks. The two synthetic hurricanes, generated by FEMA, were simulated in *ADCIRC* using the Powell wind drag law to obtain maximum storm surge and wind speeds in the entire Ship Channel region (Bedient and Blackburn 2016). The two hurricanes produced approximately 100 and 250-year return period storm surges compared with historical data. The hurricane events producing 100 and 250-year-level surges are referred to as Scenarios 1 and 2, respectively.

The fragility models developed in the previous sections were used to assess the performance of ASTs under hurricane winds and storm surge. The fragility models included aleatory sources of uncertainty such as imperfections in the tank shell and uncertainties in the density of sea water. However, sources of uncertainty such as liquid level (L) and relative density of contents (ρ_l), which are epistemic in nature, were propagated by convolving the fragility functions with assumed probability density functions (PDF). Because determination of actual level of liquid in each of the tanks during a hurricane was not possible, the liquid level in each tank was assumed to uniformly vary between zero and 90% of tank height; 10% of the capacity is usually reserved for overflow protection. The database of tank information provides a range for the expected relative density of contents stored in the tanks, which may range from 0.5 to 1.0 depending on the contents. The relative density of contents was assumed to be uniformly distributed within the provided range. However, this assumption may be relaxed in the future if precise information on the contents and their density becomes available. Using these assumptions, the fragility of tanks can be obtained as

$$P(failure|IM,\mathbf{X}) = \iint P(failure|IM,\mathbf{X},l,\rho) f_L(l) f_{\rho_l}(\rho) dl \cdot d\rho \tag{6}$$

where $P(failure|IM,\mathbf{X},l,\rho)$ = logistic regression model for a particular failure mode; IM = corresponding intensity measure, such as wind speed for wind buckling; $\mathbf{X}$ = vector of tank dimensions; and $f_L(l)$, and $f_{\rho_l}(\rho)$ = PDFs of liquid height and relative density. Eq. (6) was evaluated using Monte Carlo simulations with 100,000 simulations. Additionally, the distribution of repair costs, downtime, and spill volumes were also obtained using MCS.

The aforementioned approach was first applied to assess the effects of hurricane winds on ASTs in the Ship Channel for the two scenarios. The maximum wind speeds at the tank locations for the Scenarios 1 and 2 were 39.15 and 46.85 m/s, respectively; minor local variations of approximately 2–3 m/s in wind speeds were observed depending on the location of tanks. For both scenarios, the failure probabilities, i.e., probability of tank buckling, for all tanks were very low, less than 5%. Such low failure probabilities may be attributed to two main reasons. First, the two hurricanes did not produce very high wind speeds in the Ship Channel; the wind speeds were lower than the 25-year return period winds. Secondly, the tanks are designed to resist hurricane winds because the design guidelines mandate several measures such as the use of stiffening rings to prevent wind buckling. For comparison, the fragility of all tanks for a 300-year return period wind speed were also evaluated assuming constant wind speed for all tanks. Again, low buckling probabilities, less than 5%, were observed, which shows the effectiveness of the buckling prevention measures mandated by design guidelines. Based on these results, it may be concluded that hurricane winds do not generally pose a significant threat to the integrity of ASTs in the Ship Channel.

Next, using the procedure described to assess performance under hurricane winds, the performance of ASTs subjected storm surge was evaluated for the two synthetic hurricane scenarios. For storm surge–related failures, a series system assumption was adopted for the two failure modes; i.e., tanks were assumed to fail if they fail due to either flotation or buckling. Furthermore, all tanks were assumed to be unanchored; this assumption is reasonable because design guidelines do not mandate anchoring of tanks for storm surge–related loads. With these assumptions, the failure probabilities of all of the ASTs in the HSC were evaluated for the two scenarios. Figs. 6(a and b) show the location of all tanks, failure probability for each tank, and the extent of storm surge inundation. The range of inundation levels for Scenario 1 [Fig. 6(a)] was from 0 to 6.85 m and that for Scenario 2 was 0–8.18 m [Fig. 6(b)]. In Fig. 6, the background shows areal imagery of the Houston region, obtained from *ArcGis*; the dots represent tanks and their shading indicates the probability of failure. For Scenario 1, four regions, R1–R4, were identified; Regions R1 and R4 had a large number of tanks with significant failure probability, but very few tanks had more than a 75% chance of failure. Regions R2 and R3 had fewer tanks, but include those tanks with very high failure probability. In Scenario 2, as the inundation extended landward, more tanks had nonzero failure probability. In addition to the four regions identified for Scenario 1, another region, R5, with a large number of tanks having significant (although not extremely high) failure probability was identified. The four regions, R1–R4, had low ground elevation, which led to higher inundation levels and consequently higher failure probabilities; however, Region R5, which was at a relatively higher elevation, had a large number of tanks with nonzero failure probability due to the large extent of storm surge inundation.

Comparison of wind and surge performance of ASTs clearly highlights that ASTs in the Ship Channel are more vulnerable to storm surge. This observation can be primarily attributed to the design guidelines, which require tanks to be designed to resist high wind speeds, but the same guidelines do not mandate any measures to prevent surge-related failure. Furthermore, the measures for prevention of wind buckling do not improve the storm surge performance. For example, the in case of flotation, the additional weight due to the stiffening rings that prevent wind buckling is negligible compared with the buoyancy forces; therefore wind buckling prevention measures do not prevent storm surge flotation. Wind buckling prevention strategies are also ineffective in preventing storm surge buckling of ASTs because the buckling behavior of ASTs is different under wind and storm surge loads; buckling caused by wind loads occurs in the upper shell courses, whereas in case of storm surge the lower shell courses buckle. This difference

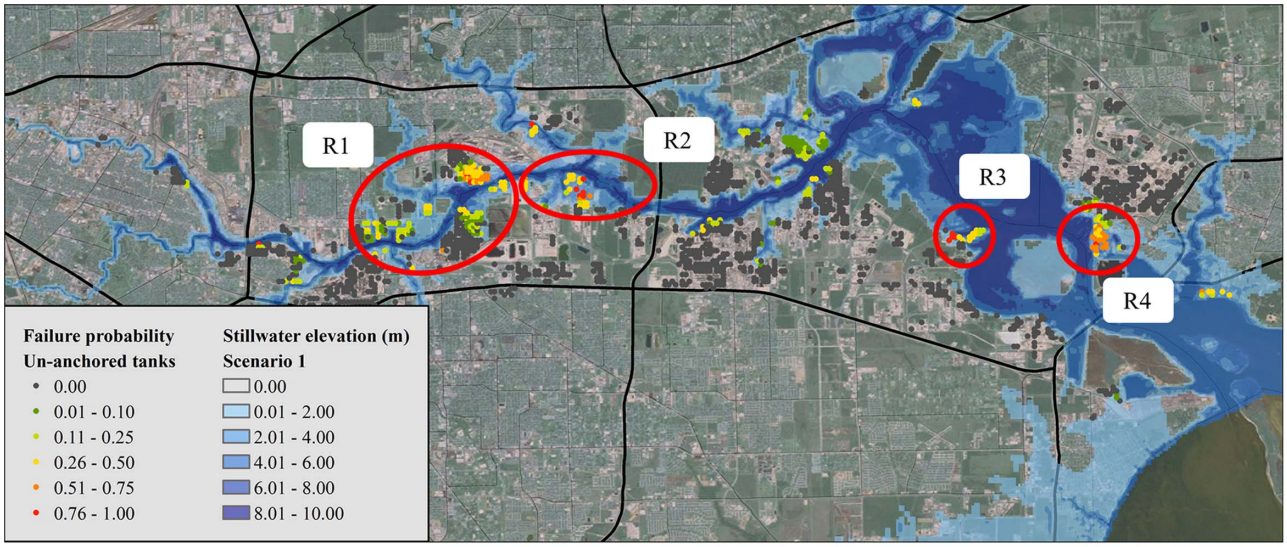

(a)

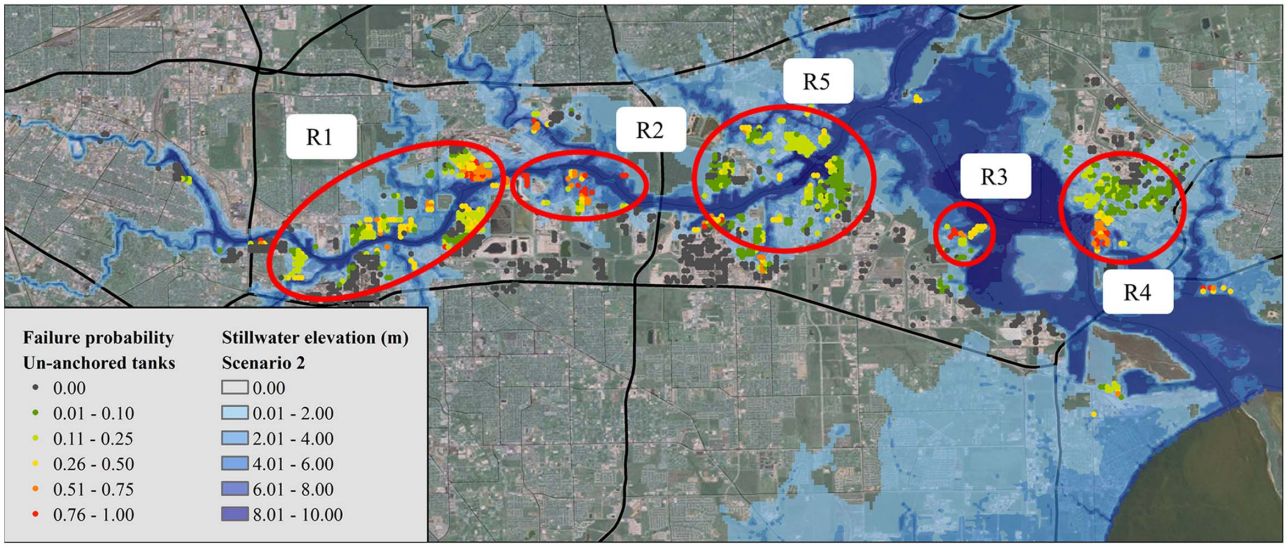

(b)

Fig. 6. Storm surge failure probabilities: (a) Scenario 1; (b) Scenario 2

in buckling behavior renders wind girders (located in the upper shell courses) ineffective in preventing storm surge buckling. Because tanks are vulnerable to surge-related failures, and measures for other hazards are not sufficient to prevent surge failures, the design guidelines need provisions to prevent storm surge–related failures.

Because a large number of tanks were observed to have nonzero failure probability, this study further evaluated the resilience indicators for ASTs in the ship channel. Use of MCS allows examination of the PDFs of each of the resilience metrics, which revealed an interesting insight. Fig. 7 shows the normalized histogram of repair costs for a single AST. For a large number of simulations, zero costs were observed, which resulted in a spike at zero; the nonzero repair costs were clustered around \$1.1–\$1.4 million. If the tank did not fail, it did not incur any repair cost. Therefore the spike at zero corresponds to the probability of survival, and the costs around \$1 million were for the cases that failed during MCS. Similar trends were observed for repair costs, downtime, and spill volumes for all other tanks with nonzero failure probability. This observation suggests that expected values may not effectively communicate the magnitude of repair costs in the case of failure. Therefore this study also evaluated mean values of resilience indicators conditioned on failure, i.e., the mean value of indicators for cases in which the tank fails. However, communicating conditional mean values alone may be misleading for some decision makers because it excludes the cases in which the tank survives, and therefore leads to high values. For this reason, both expected values and the conditional mean vales are shown; the expected values can highlight tanks which can be expected to have high values for repair costs and other resilience indicators, and the conditional mean can show the extent of values that can be expected in the case of tank failure.

Figs. 8(a and b) and 9(a and b) show the expected and the conditional mean value of repair costs for Scenarios 1 and 2, respectively. Figs. 8(b) and 9(b) only show the conditional repair costs for tanks which have nonzero failure probability. In Fig. 8(a), Regions R1, R3, and R4 have significant repair costs; although Region R2 has tanks with very high failure probability, the region does not have high repair costs. Similar observations can be made from Fig. 9(a), in which R1, R3, and R4 have tanks with high repair costs, whereas R2 and R5 do not have high repair costs in spite of having tanks

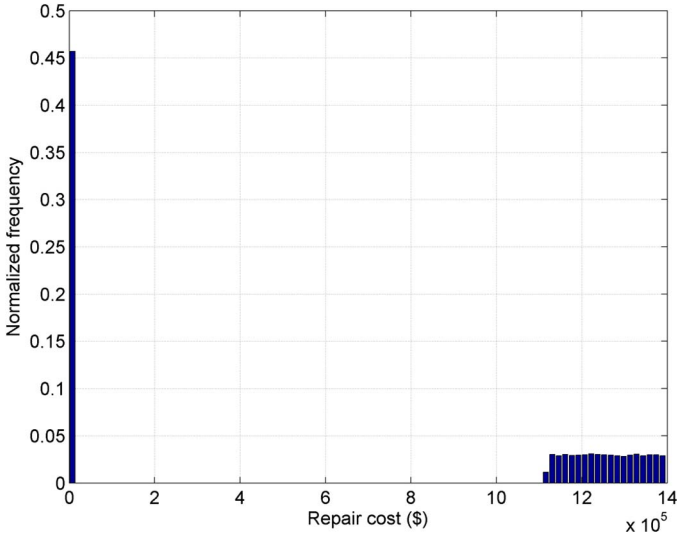

Fig. 7. Histogram of repair costs for an example tank

with significant failure probability. This observation suggests that tanks with the highest failure probabilities are not necessarily those with the highest expected value of repair costs. This trend is caused by the size of tanks; the tanks in Regions R2 and R5 are relatively smaller and therefore their repair costs are lower. Fig. 8(a) can help identify regions in which high repair costs can be expected; Figs. 8(b) and 9(b) show the mean values of repair costs if tanks in these regions fail. Different values of conditional repair costs can be observed for tanks within the same region and across different regions. The disparity in repair costs can be attributed the difference in their sizes, which leads to different replacement costs and consequently repair costs.

Figs. 10 and 11 show expected downtime estimates for Scenarios 1 and 2, respectively. The downtime estimates were highly dependent on failure probabilities shown in Fig. 6. For all tanks with nonzero failure probability, the conditional mean values of downtime were close to 160 days. This observation suggests that storm surge failure of ASTs is mostly dominated by floatation failure, because the mean downtime for flotation failure is 155 days.

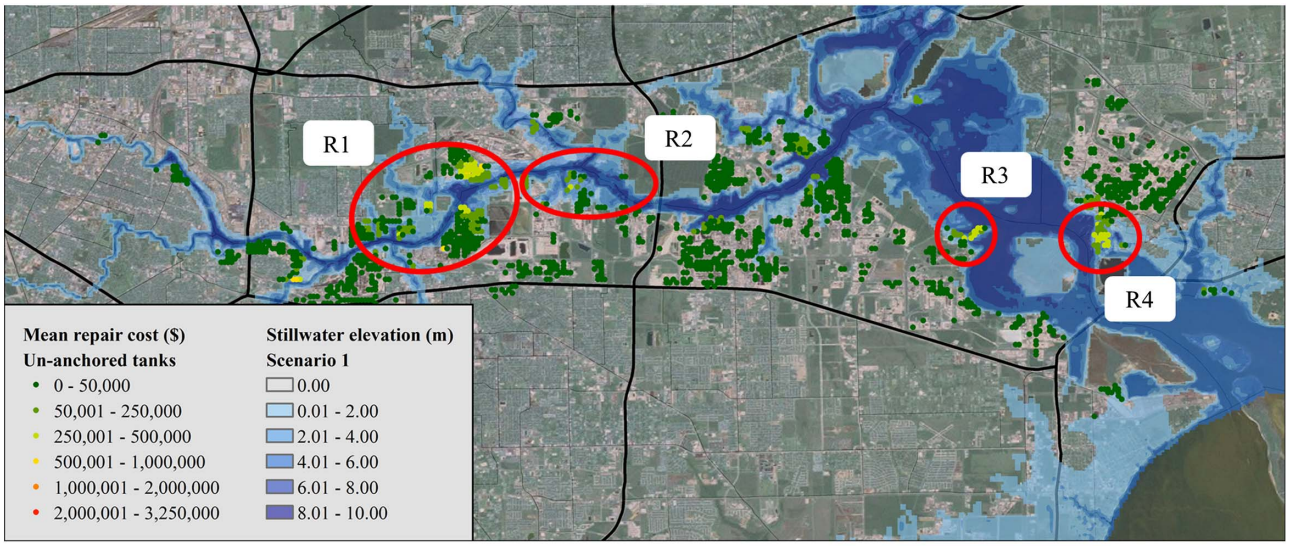

(a)

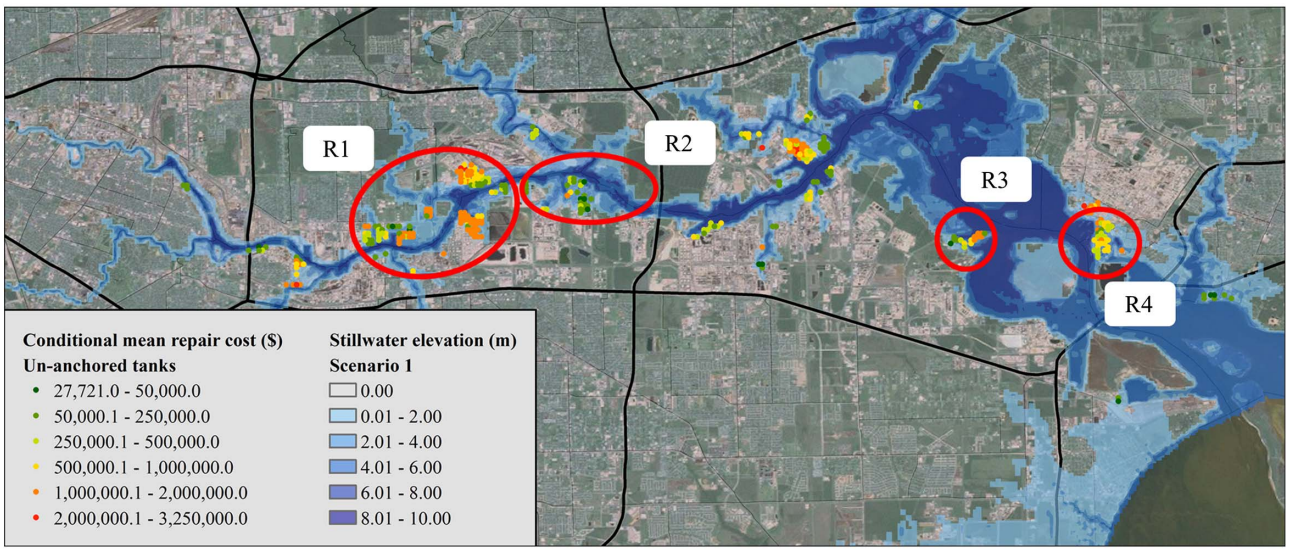

(b)

Fig. 8. Scenario 1: (a) mean repair costs; (b) conditional mean repair cost

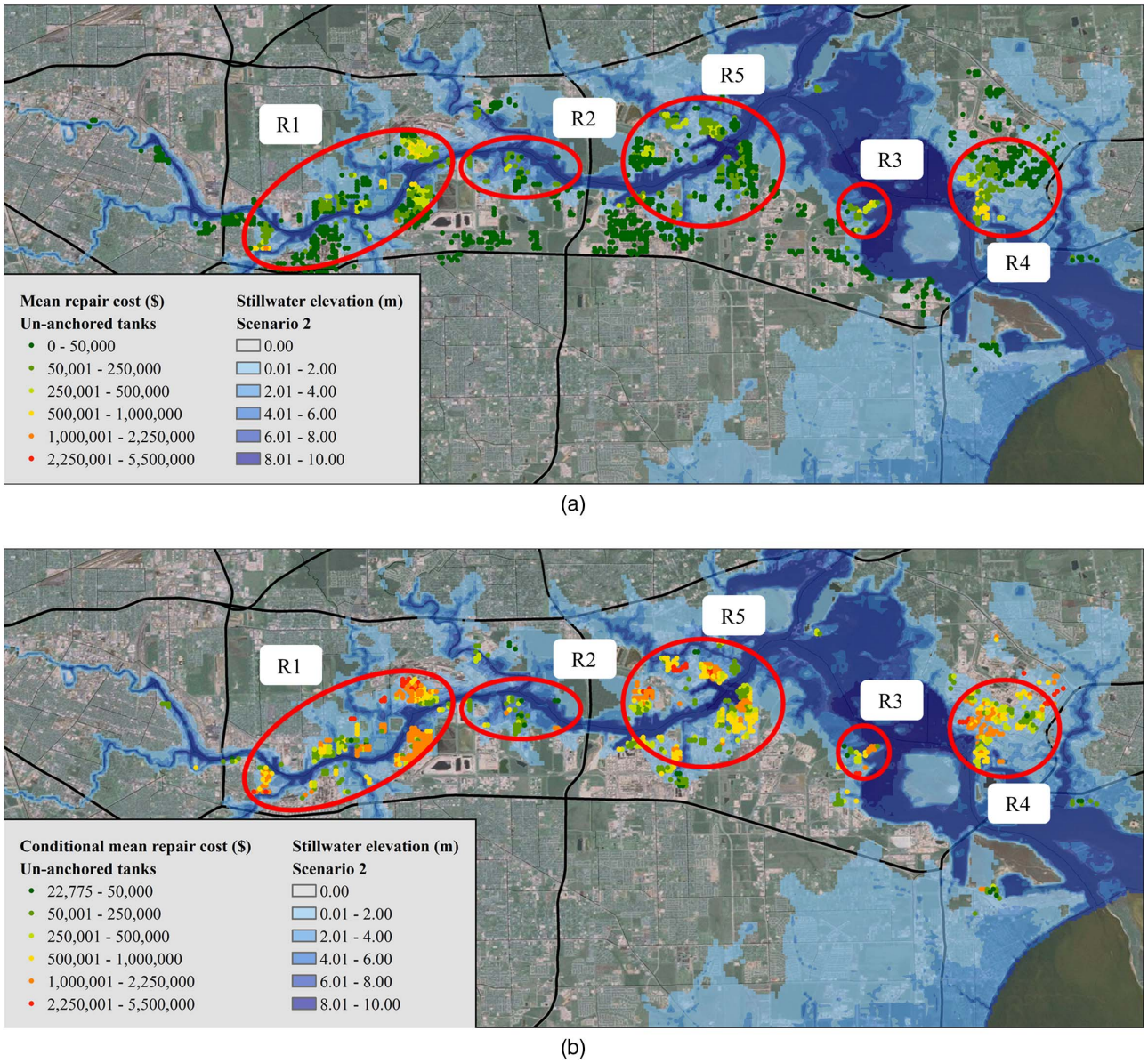

Fig. 9. Scenario 2: (a) mean repair costs; (b) conditional mean repair cost

Figs. 12(a and b) and 13(a and b) show expected values and conditional mean values of spill volumes (i.e., expected value of spill volume given that the tank has failed) for the respective scenarios. The trends in spill volume and repair costs were very similar; regions with high failure probability did not always have high spill volumes. Figs. 12(a) and 13(a) identify the regions that may have high spills and Figs. 12(b) and 13(b) show the magnitude of possible spills for each tank.

Spills can have long-term environmental and societal effects. Moreover, failure of ASTs and consequent spills would lead to disruption of the economic activity in the Ship Channel. Clean-up of 1 m^3 of oil spill alone can cost $39,000 in 1999 U.S. dollars (Etkin 2000). Clean up costs for the entire Ship Channel region may lead to excessive economic losses. Therefore this study evaluated the effect of a structural mitigation measure—anchoring tanks—on the performance of ASTs in the Ship Channel. For this purpose, as an illustration, anchors were assumed to be provided at a spacing of 3.0 m, which is the maximum allowed spacing according to API 650 (API 2013) seismic design provisions. Using appropriate fragility functions from previous sections, the failure probability of anchored ASTs subjected to storm surge was assessed again for the two scenarios. Performance assessment of tanks under hurricane winds was not repeated because the anchoring of tanks does not influence the buckling performance of ASTs under hurricane winds. For brevity, maps showing the results for every tank in the Ship Channel are not shown; however, Table 4 presents collective results—the mean and coefficient of variation (COV) of total repair costs and spill volumes for unanchored and anchored cases for all of the ASTs in Ship Channel. Additionally, Table 4 also shows the percentage reduction in repair costs and spill volume due to anchoring with respect to the unanchored case. For both scenarios, even minimal anchoring leads to approximately 40% reduction in mean values of total repair costs and spill volumes compared with unanchored tanks, with minor changes in COV. Therefore anchoring of tanks can be considered as a potential mitigation measure to improve the performance of ASTs at the structural level. Further reduction in the repair costs and spill volumes can be achieved by increasing the anchoring for tanks by reducing

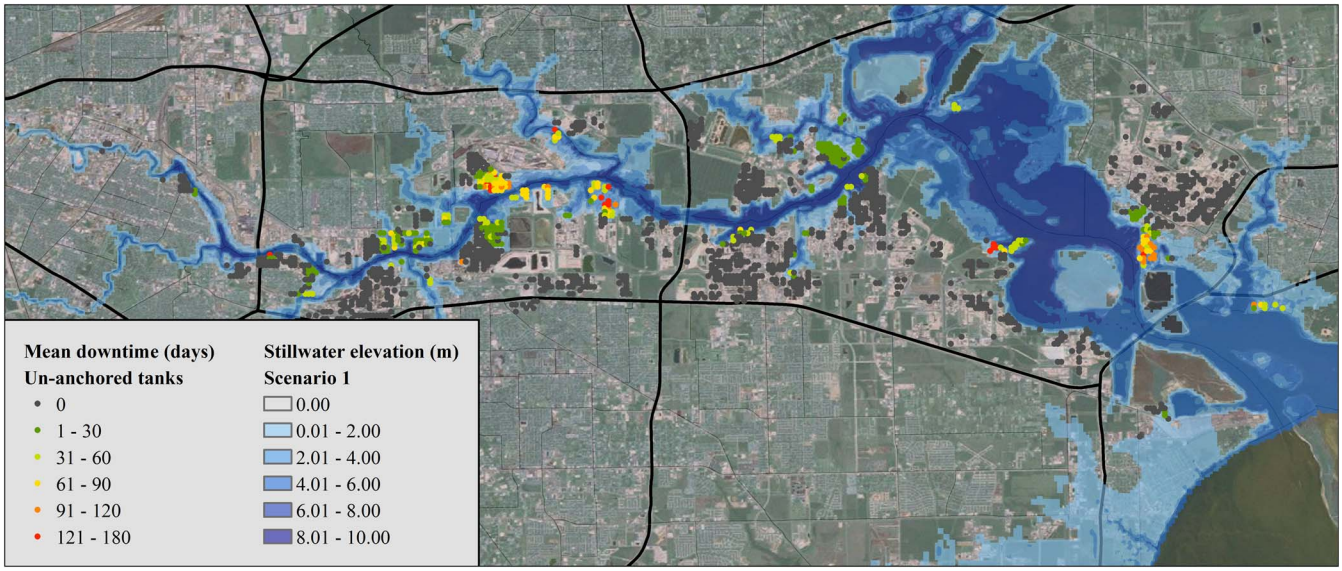

Fig. 10. Expected downtime for tanks in Scenario 1

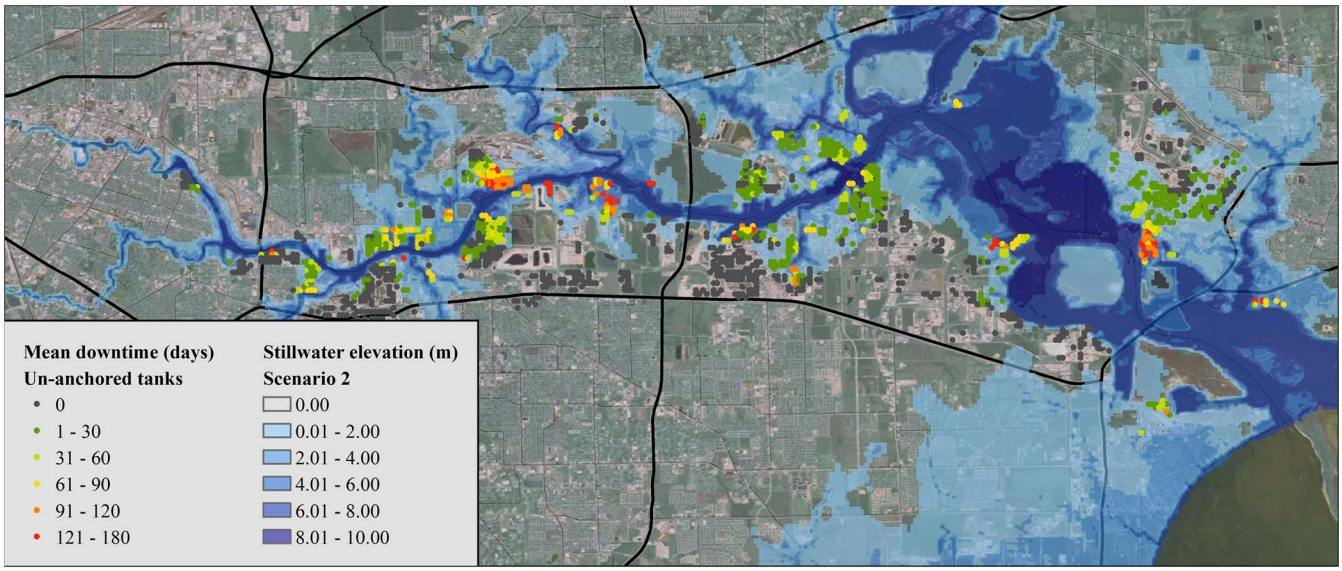

Fig. 11. Expected downtime for tanks in Scenario 2

the anchor spacing. However, excessive anchoring may lead to storm surge buckling failures instead of flotation failures. Therefore optimal anchoring may be provided to maximize the performance of ASTs; optimization of repair costs can be facilitated by the fragility functions and the resilience indicators developed in this study. Future work may focus on deriving such optimal mitigation measures based on regional-level resilience indicator targets.

Conclusions

This study facilitated probabilistic performance assessment of a regional portfolio of aboveground storage tanks subjected to hurricane-related hazards such as wind and storm surge. For this purpose, this study derived fragility functions for ASTs and developed estimates for repair costs, downtime, and spill volumes for tanks damaged by hurricane wind and storm surge. First, this study derived fragility functions to predict wind buckling of ASTs subjected to hurricane winds, which are lacking in the literature, and parameterized them for application to a regional portfolio. Additionally, this study also developed buckling fragility models for ASTs with floating roofs subjected to wind and storm surge, which are also lacking in the existing literature. The final fragility models for floating-roof tanks show that the stiffness of the rim seal of the floating roof does not have a significant effect on the buckling fragility of ASTs for both wind and storm surge given the other sources of variation such as tank imperfections. Fragility comparisons were also presented for a case study tank with fixed and floating roof for wind and storm surge buckling, which showed that the presence of a floating roof may influence wind buckling significantly more than it influences storm surge buckling.

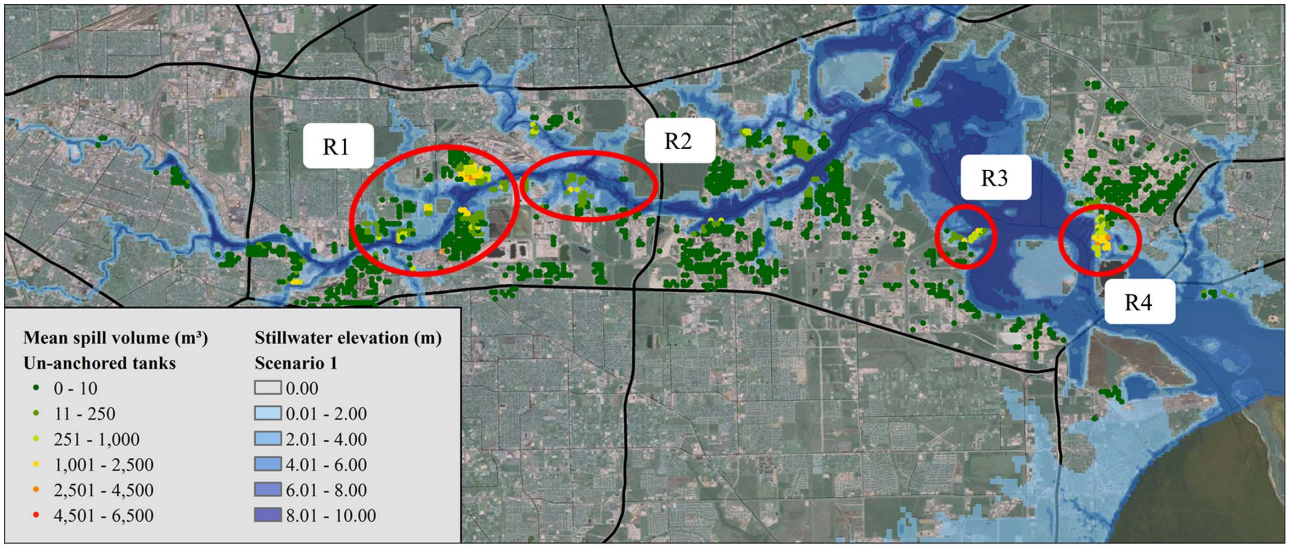

(a)

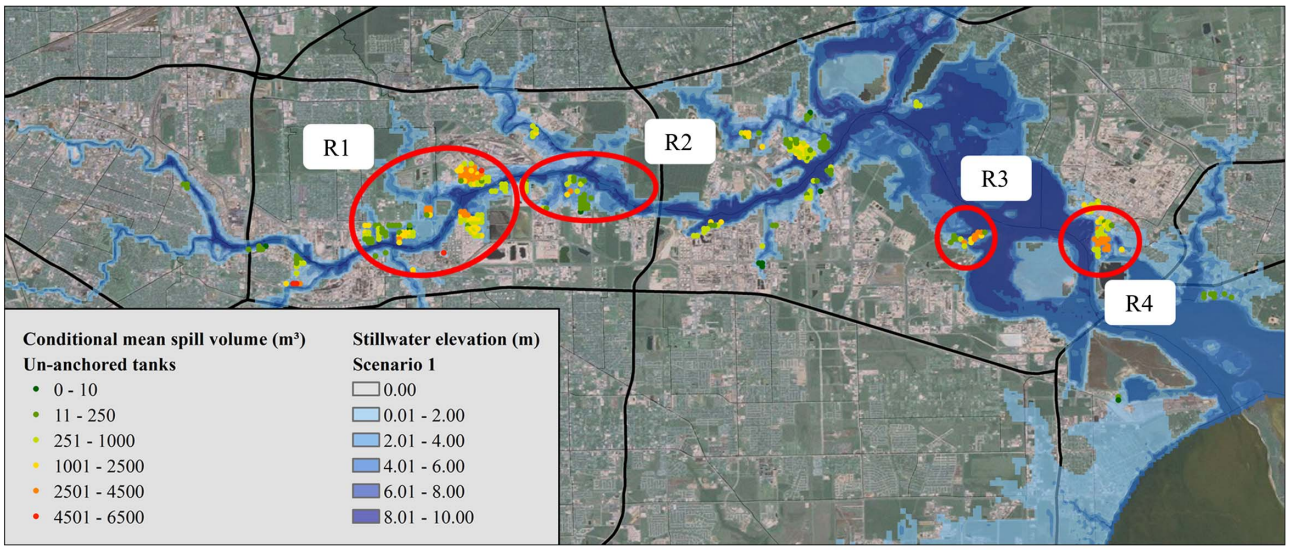

(b)

Fig. 12. Scenario 1: (a) mean spill volumes; (b) conditional mean spill volumes

In addition to fragility functions, this study also developed estimates for resilience indicators of ASTs. Conventionally, infrastructure resilience is measured using the area under the time-evolving functionality curve. However, due to the binary functionality states of ASTs—fully functional or completely closed—this study suggests that downtime of ASTs can serve as a good indicator or proxy for resilience. Therefore this study developed estimates for downtime of ASTs for various failure modes. Additionally, repair cost estimates were also developed for ASTs damaged due to different failure modes. Because such estimates are not available for ASTs damaged during hurricanes, the damage to tanks due to hurricane wind and storm surge was compared with seismic damage to tanks to identify similar damage levels and consequences, and therefore to identify repair cost and downtime models. Furthermore, spill volumes for tanks were also evaluated assuming that the entire contents of tanks were spilled during flotation failure and storm surge buckling that led to shell rupturing. The fragility models and the estimates of downtime and repair costs were used to determine the hurricane performance of the regional portfolio of ASTs in the largest petrochemical facility in the United States, the Houston Ship Channel, for two synthetic storms which produce storm surge levels that approximately correspond to 100 and 250-year events. The results of the portfolio analysis of tanks provide several insights into the performance of ASTs during hurricanes. The results suggest that the ASTs in the Ship Channel have very low probability of buckling due to hurricane winds. In contrast to hurricane winds, however, ASTs are not designed for storm surges; therefore, high probabilities of failure were observed due to storm surge for the two hurricane scenarios. Analysis of the distributions of repair costs and spill volumes show that mean values are not sufficient to communicate the potential values of spills and repair costs on a per-tank basis. Therefore this study evaluated mean estimates of resilience indicators conditioned on failure, i.e., expected values in the event of failure. However, first-order and second-order moments of the total repair costs and spill volumes of all the tanks can be used to study the collective performance of the regional portfolio of ASTs. Analysis of failure probabilities and resilience indicators showed that, due to variations in dimensions, tanks with

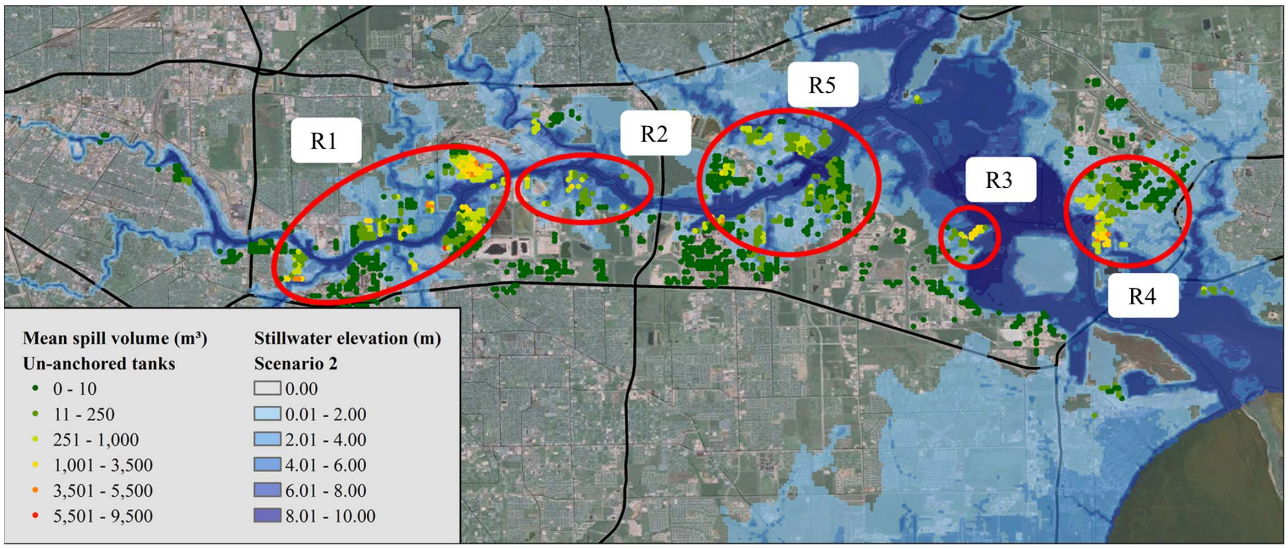

(a)

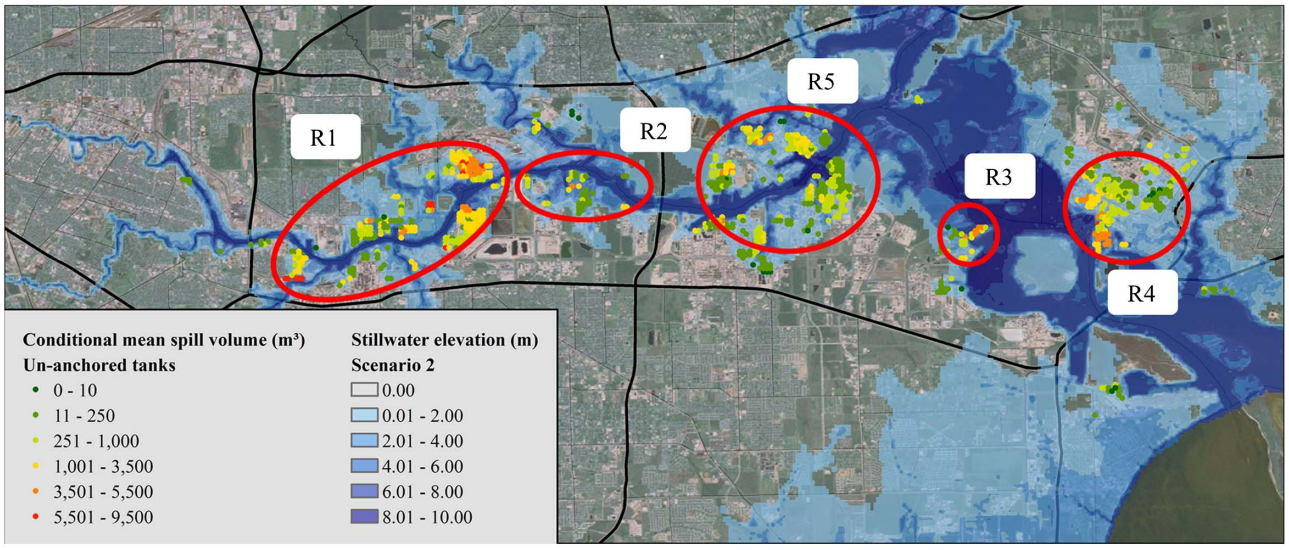

(b)

Fig. 13. Scenario 2: (a) mean spill volumes; (b) conditional mean spill volumes

Table 4. Comparison of Mean and COV of Total Repair Costs and Spill Volume

Hurricane scenario	Unanchored tanks		Anchored tanks		% difference between mean values for unanchored and anchored ASTs
	Mean	COV	Mean	COV	
Total repair costs ($)					
Scenario 1	83.89×10^6	8.15×10^{-2}	52.63×10^6	11.63×10^{-2}	37.3
Scenario 2	217.29×10^6	5.04×10^{-2}	137.38×10^6	7.75×10^{-2}	36.8
Total spill volume (m^3)					
Scenario 1	20.01×10^4	10.61×10^{-2}	11.89×10^4	14.53×10^{-2}	40.6
Scenario 2	52.52×10^4	7.07×10^{-2}	33.41×10^6	9.43×10^{-2}	36.4

the high failure probability may not necessarily cause the largest spills or lead to the highest repair costs. Furthermore, the results showed that for both hurricane scenarios, many tanks were vulnerable to flotation failure, which highlights the need for either structural or regional surge mitigation strategies. In view of this, the effect of anchoring was studied as a structural mitigation strategy. Comparison of total spill volumes and repair costs for the entire Ship Channel for unanchored and anchored tanks revealed that even minimal anchoring is effective in reducing the mean repair costs and mean spill volumes for both hurricane scenarios by 40%. The fragility models and the estimates for resilience indicators developed in this study can facilitate assessment of mitigation strategies at a regional and structural level. Furthermore, the contributions of this study may also facilitate future studies on lifecycle

performance assessment of ASTs subjected to hurricanes. Future work may also focus on including other failure modes such as wave effects or debris impact for performance assessment of ASTs during storm surge events.

Acknowledgments

The authors acknowledge the support for this research by the Houston Endowment and by the National Science Foundation (NSF) under Grant No. CMMI-1635784. Any opinions, findings, and conclusions or recommendations expressed herein are those of the authors and do not necessarily reflect the views of the funding agencies. The authors also acknowledge computational facilities provided by Data Analysis and Visualization Cyberinfrastructure (NSF Grant No. OCI-0959097).

References

ADCIRC version 51 [Computer software]. Univ. of North Carolina at Chapel Hill, Chapel Hill, NC.

API (American Petroleum Institute). (2013). "Welded steel tanks for oil storage." *API 650*, Washington, DC.

ArcGIS version 10 [Computer software]. ESRI, Redlands, CA.

Barton, D., and Parker, J. (1987). "Finite element analysis of the seismic response of anchored and unanchored liquid storage tanks." *Earthquake Eng. Struct. Dyn.*, 15(3), 299–322.

Bedient, P., and Blackburn, J. (2016). "Developing a Houston-Galveston area protection system (HGAPS)—SSPEED center update." SSPEED Center, Rice Univ., Houston.

Berkeley, A. R., III, and Wallace, M. (2010). *A framework for establishing critical infrastructure resilience goals*, National Infrastructure Advisory Council, Washington, DC.

Bernier, C., Elliott, J. R., Padgett, J. E., Kellerman, F., and Bedient, P. B. (2017). "Evolution of social vulnerability and risks of chemical spills during storm surge along the Houston Ship Channel." *Nat. Hazards Rev.*, 10.1061/(ASCE)NH.1527-6996.0000252, 04017013.

Bruneau, M., et al. (2003). "A framework to quantitatively assess and enhance the seismic resilience of communities." *Earthquake Spectra*, 19(4), 733–752.

Cozzani, V., Campedel, M., Renni, E., and Krausmann, E. (2010). "Industrial accidents triggered by flood events: Analysis of past accidents." *J. Hazard. Mater.*, 175(1), 501–509.

Cristianini, N., and Shawe-Taylor, J. (2000). *An introduction to support vector machines and other kernel-based learning methods*, Cambridge University Press, Cambridge, U.K.

CEN (European Committee for Standardization). (2007). "Design of steel structures—Part 4-1: Design of steel structures: Silos." *EN 1993-4-1 Eurocode 3*, Brussels, Belgium.

EPA. (2016). "Flood preparedness—Recommended best practices." *Regional Response Team 6 Fact Sheet #103a*, Dallas.

Etkin, D. S. (2000). "Worldwide analysis of marine oil spill cleanup cost factors." *Proc., Arctic and Marine Oilspill Program Technical Seminar*, Environment Canada, Ottawa, 161–174.

Fabbrocino, G., Iervolino, I., Orlando, F., and Salzano, E. (2005). "Quantitative risk analysis of oil storage facilities in seismic areas." *J. Hazard. Mater.*, 123(1–3), 61–69.

Flores, F. G., and Godoy, L. A. (1998). "Buckling of short tanks due to hurricanes." *Eng. Struct.*, 20(8), 752–760.

Godoy, L. (2007). "Performance of storage tanks in oil facilities damaged by Hurricanes Katrina and Rita." *J. Perform. Constr. Facil.*, 10.1061/(ASCE)0887-3828(2007)21:6(441), 441–449.

Godoy, L. A., and Flores, F. G. (2002). "Imperfection sensitivity to elastic buckling of wind loaded open cylindrical tanks." *Struct. Eng. Mech.*, 13(5), 533–542.

Hallquist, J. O. (2012). *LS-DYNA keyword user's manual*, Livermore Software Technology, Livermore, CA.

Haroun, M. A., and Housner, G. W. (1981). "Earthquake response of deformable liquid storage tanks." *J. Appl. Mech.*, 48(2), 411–418.

Hosmer, D., and Lemeshow, S. (1989). *Applied logistic regression*, Wiley, New York.

Hosseini, M., Soroor, A., Sardar, A., and Jafarieh, F. (2011). "A simplified method for seismic analysis of tanks with floating roof by using finite element method: Case study of Kharg (southern Iran) Island tanks." *Proc. Eng.*, 14, 2884–2890.

Kameshwar, S., and Padgett, J. (2015a). "Stochastic modeling of geometric imperfections in aboveground storage tanks for probabilistic buckling capacity estimation." *ASCE-ASME J. Risk Uncertain. Eng. Syst., Part A: Civ. Eng.*, 2(2), C4015005.

Kameshwar, S., and Padgett, J. E. (2015b). "Fragility assessment of above ground petroleum storage tanks under storm surge." *Proc., 12th Int. Conf. on Applications of Statistics and Probability in Civil Engineering*, Univ. of British Columbia, Vancouver, Canada.

Kameshwar, S., and Padgett, J. E. (2018). "Storm surge fragility assessment of above ground storage tanks." *Struct. Saf.*, 70, 40–48.

Kingston, P. F. (2002). "Long-term environmental impact of oil spills." *Spill Sci. Technol. Bull.*, 7(1–2), 53–61.

LS-DYNA version 8.0 [Computer software]. LSTC, Livermore, CA.

Luettich, R. A., and Westerink, J. J. (2004). "Formulation and numerical implementation of the 2D/3D ADCIRC finite element model version 44. XX." Univ. of North Carolina at Chapel Hill, Chapel Hill, NC.

Maki, A. W. (1991). "The Exxon Valdez oil spill: Initial environmental impact assessment. Part 2." *Environ. Sci. Technol.*, 25(1), 24–29.

Michigan Department of Treasury. (2003). "Assessor's manual volume II." State of Michigan, Lansing, MI.

Myers, P. E. (1997). *Aboveground storage tanks*, McGraw-Hill, New York.

NBCNews.com. (2006). "$330 million settlement deal in Katrina oil spill." ⟨http://www.nbcnews.com/id/15004868/ns/us_news-environment/t/million-settlement-deal-katrina-oil-spill/#.VeWtoPlViko⟩ (Sep. 1, 2015).

Nelson-Farrar Refinery Construction Index. (2004). *Oil and gas journal*, Vol. 102, PennWell Petroleum Group, Tulsa, OK.

Nelson-Farrar Refinery Construction Index. (2016). *Oil and gas journal*, Vol. 114, PennWell Petroleum Group, Tulsa, OK.

NIBS (National Institute of Building Sciences). (2005). "Multi-hazard loss estimation methodology, earthquake model, HAZUS® MH technical manual." Washington, DC.

Niwa, A., and Clough, R. W. (1982). "Buckling of cylindrical liquid-storage tanks under earthquake loading." *Earthquake Eng. Struct. Dyn.*, 10(1), 107–122.

O'Rourke, M. J., and So, P. (2000). "Seismic fragility curves for on-grade steel tanks." *Earthquake Spectra*, 16(4), 801–815.

Palinkas, L., Downs, M., Petterson, J., and Russell, J. (1993). "Social, cultural, and psychological impacts of the Exxon Valdez oil spill." *Hum. Organ.*, 52(1), 1–13.

Pavlov, Y. L. (2000). *Random forests*, VSP, Zeist, Netherlands.

Portela, G., and Godoy, L. A. (2005a). "Wind pressures and buckling of cylindrical steel tanks with a conical roof." *J. Constr. Steel Res.*, 61(6), 786–807.

Portela, G., and Godoy, L. A. (2005b). "Wind pressures and buckling of cylindrical steel tanks with a dome roof." *J. Constr. Steel Res.*, 61(6), 808–824.

Sakai, F., Nishimura, M., and Ogawa, H. (1984). "Sloshing behavior of floating-roof oil storage tanks." *Comput. Struct.*, 19(1–2), 183–192.

Salzano, E., Iervolino, I., and Fabbrocino, G. (2003). "Seismic risk of atmospheric storage tanks in the framework of quantitative risk analysis." *J. Loss Prev. Process Ind.*, 16(5), 403–409.

Teng, J. G., and Rotter, J. M. (2006). *Buckling of thin metal shells*, Spon Press, London.

The Port of Houston Authority. (2016). "Overview." ⟨http://porthouston.com/about-us/⟩. (Sep. 15, 2016).

Virella, J. C., Godoy, L. A., and Suárez, L. E. (2003). "Influence of the roof on the natural periods of empty steel tanks." *Eng. Struct.*, 25(7), 877–887.

Zhao, Y., and Lin, Y. (2014). "Buckling of cylindrical open-topped steel tanks under wind load." *Thin Walled Struct.*, 79(1), 83–94.